arXiv:1605.02642v1 [cond-mat.quant-gas] 9 May 2016

Out-coupling vector solitons from a BEC with time-dependent interatomic forces

David Feijoo, Ángel Paredes and Humberto Michinel
[1] *Área de Óptica, Facultade de Ciencias de Ourense, Universidade de Vigo, As Lagoas s/n, Ourense, ES-32004 Spain.*

We discuss the possibility of emitting vector solitons from a two-component elongated BEC by manipulating in time the inter- or intra-species scattering lengths with Feshbach resonance tuning. We present different situations which do not have an analogue in the single species case. In particular, we show vector soliton out-coupling by tuning the interspecies forces, how the evolution in one species is controlled by tuning the dynamics of the other, and how one can implement the so-called supersolitons. The analysis is performed by numerical simulations of the one-dimensional Gross-Pitaevskii equation. Simple analytic arguments are also presented in order to give a qualitative insight.

PACS numbers: 03.75Lm, 42.65.Jx, 42.65.Tg

I. INTRODUCTION

Since its discovery in 1995 [1], the Bose-Einstein condensate (BEC) has been a field which has attracted a large amount of research effort both from the experimental and theoretical fronts. Among many interesting research tracks, the design of cold atom interferometers stands as an exciting possibility [2]. The external control of the condensed atomic clouds is a key factor for any such application. This fact highlights the importance of the theoretical understanding of atom manipulation protocols and, of course, of their experimental implementation.

Bright solitons are bunches of energy or matter whose shape does not change upon propagation, due to non-linear effects. They have been discussed in very different contexts such as quantum field theory or non-linear optics and were first observed in the frame of BECs in [3, 4]. The fact that solitons remain robust and undistorted makes them interesting for the goal of building precise matter-wave interferometers [5]-[13]. It is well known that they can only be stable in one-dimensional settings and for that reason we will concentrate in elongated traps such the dynamics can be effectively reduced to a line [14]. In creating such solitary waves, it is essential to have inter-atomic attractive forces. The tuning of Feshbach resonances [15] — see [16] for a review — is instrumental for this purpose: the scattering length of atom-atom collisions drastically changes when colliding atoms couple resonantly to a molecular bound state, and this can be externally controlled by lasers and/or magnetic fields.

The present theoretical contribution introduces protocols of atom manipulation that can be useful in this framework. Ways of out-coupling self-trapped matter from a shallow potential in a coherent manner are discussed. There are many previous works following similar strategies, but we will focus in the possibility of working with time-dependent interactions [17] in multicomponent BECs, which allows a high degree of control over the number and properties of the emitted soliton pairs [13]. In fact, this paper is a natural generalization of [13], extending the discussion to phenomena constrained to multicomponent BECs. Solitary waves in which different fields are involved in producing the self-trapping are called vector solitons. They were first studied by Manakov in the context of non-linear optical fibers [18], and have been thoroughly discussed for BECs, see for instance [19–21] and references therein. It is important to notice that the Feshbach resonance tuning technique has been experimentally accomplished in multicomponent condensates [22].

In section II, we fix notation and present the Gross-Pitaevskii equations (GPEs) used for the analysis. In sections III-V, we discuss, by numerically solving the evolution equations, manipulations that allow to out-couple solitonic excitations from a shallow trap in which a two-component BEC is initially confined. The general scheme underlying the different protocols is the following: first, strong inter-atomic repulsion is induced such that part of atomic cloud is pushed out of the trap. Then, by tuning again the internal forces, a instability is produced, eventually leading to the formation of the desired structures. We study different situations in which the multicomponent nature of the condensate is essential, not having an analogue in the single species case. In particular, in section III we show how the process can be carried out by tuning the *interspecies* scattering length. In section IV, we demonstrate how one species can be indirectly manipulated by tuning the intra-species interaction of the other one. In section V, we analyse how a so-called super-solitonic excitation [23] can be obtained in the same framework.

It is worth noticing that very interesting phenomena also occur when the two species in the condensate are different hyperfine states of the same alkali atom. In that case, it is possible to implement Rabi couplings with an external laser beam in order to transfer atoms from one species to the other one [24]. However, we will not explore this possibility in the present work.

II. GPES AND INITIAL CONDITIONS

The zero temperature mean-field theory description of a collection of identical bosons is the Gross-Pitaevskii equation [25]. For a multicomponent BEC, there is a coupled system of equations for the evolution of the atom densities of the different elements:

$$i\,\hbar\frac{\partial\Psi_i}{\partial t} = -\frac{\hbar^2}{2m_i}\nabla^2\Psi_i + V_i\,\Psi_i + U_{ij}|\Psi_j|^2\Psi_i \qquad (1)$$

where m_i corresponds to the mass of the i'th species, the V_i are external potentials and the $U_{ij} = 2\pi\,\hbar^2 a_{ij}/m_{ij}$ parameterize the inter-atomic forces in terms of the s-wave scattering lengths and the reduced masses $m_{ij} = m_i m_j/(m_i + m_j)$. It is worth pointing out that this usually written expression has been challenged [26]. In any case, the precise relation between the U's and the a's is not essential for our analysis, as long as the inter-atomic forces can be externally tuned. The normalization conditions are $\int|\Psi_i|^2 d^3\vec{r} = N_i$, where N_i is the number of atoms of the corresponding species.

In this paper, cigar-shaped atomic traps will be considered: a strong potential traps the atoms in two directions and the dynamics is reduced to a quasi-one-dimensional problem. The reason is that it is in this highly asymmetric traps where stable solitons can be created [14]. In the longitudinal dimension (z) the system is weakly confined by a shallow optical dipole trap. Thus we take:

$$V_i = V_{\perp,i} + V_{z,i}(z) = \frac{1}{2}m_i\omega_{i\perp}^2(x^2+y^2) + V_{z,i}(z) \qquad (2)$$

where $V_{z,i}(z)$ is defined with a Gaussian shape characterized by a depth potential V_0 and a proper width L. In order to dimensionally reduce Eq. (1), one can write an approximate solution with separate variables:

$$\Psi_i = e^{-i\,\omega_{i\perp}t}\sqrt{\frac{m_i\omega_{i\perp}N_1}{\pi\,\hbar\,r_\perp}}\exp\left(-\frac{m_i\omega_{i\perp}}{2\hbar}(x^2+y^2)\right)\psi_i(z) \qquad (3)$$

where the length scale $r_\perp = \sqrt{\hbar/m_1\omega_{1\perp}}$ has been introduced. Multiplying Eq. (1) by Ψ_i^*, integrating out the x, y dependence and defining $\kappa = m_1/m_2$ yields, for the two-component case:

$$\begin{aligned} i\frac{\partial\psi_1}{\partial\tau} &= -\frac{1}{2}\frac{\partial^2\psi_1}{\partial\eta^2} + f_1\psi_1 + g_{11}|\psi_1|^2\psi_1 + g_{12}|\psi_2|^2\psi_1 \\ i\frac{\partial\psi_2}{\partial\tau} &= -\frac{\kappa}{2}\frac{\partial^2\psi_2}{\partial\eta^2} + f_2\psi_2 + g_{12}|\psi_1|^2\psi_2 + g_{22}|\psi_2|^2\psi_2 \end{aligned} \qquad (4)$$

A number of dimensionless quantities have been defined:

$$\tau = \omega_{1\perp}t, \qquad \eta = \frac{z}{r_\perp}, \qquad f_i = \frac{V_{z,i}}{\hbar\,\omega_{1\perp}}, \qquad (5)$$

together with:

$$g_{11} = \frac{2N_1a_{11}}{r_\perp}, \qquad g_{22} = \frac{2N_1a_{22}\gamma}{r_\perp}, \qquad g_{12} = \frac{2N_1a_{12}}{r_\perp}\frac{1+\kappa}{1+\kappa/\gamma}, \qquad (6)$$

with $\gamma = \omega_{2\perp}/\omega_{1\perp}$. The dimensional reduction leading to (4) have been used for instance in [27]. Slightly different reduction schemes have been employed in [19], [20], [21], yielding still equations (4), but with certain modifications of the relation between the physical parameters and the adimensional ones, Eqs. (6).

The new normalization conditions are:

$$\int|\psi_1|^2 d\eta = 1\ , \qquad \int|\psi_2|^2 d\eta = \frac{N_2}{N_1} \qquad (7)$$

In the absence of external potential $f_i = 0$, equations (4) have trivial η-independent stationary solutions. These solutions are perturbatively unstable under certain conditions and, in particular, their evolution can yield bunches of self-trapped matter. This modulational instability has been discussed for two-component GPEs in a series of papers [27], [28], generalizing the classical analysis of the single species case [29]. It turns out that stability requires both intraspecies scattering lengths to be positive $g_{11} > 0$, $g_{22} > 0$ whereas the interspecies interaction has to be sufficiently small $g_{12}^2 < g_{11}g_{22}$. Thus, instabilities appear for large enough interspecies interaction irrespective of its attractive or repulsive nature.

In all cases below, Gaussian traps [30, 31] will be considered:

$$f_1 = f_2 = \tilde{V}_0\left[1 - \exp\left(-\frac{\eta^2}{\tilde{L}^2}\right)\right] \equiv f \qquad (8)$$

where $\tilde{V}_0 = V_0/\hbar\omega_{1\perp}$ and $\tilde{L} = L/r_\perp$, so atoms can overcome the shallow potential and be out-coupled from the trap.

The analysis of this paper is based on Eqs. (4). The initial conditions for the subsequent time evolution will be given by a collection of atoms confined in the shallow trap. In order to introduce sensible initial conditions, we will use a variational approach within the Thomas-Fermi (TF) approximation, which amounts to neglecting the η-derivative terms in (4). It is known that the TF approximation yields less accurate results for the multicomponent BEC than for the single species one [32]. Nevertheless, since the stationary ground state is not our main matter of concern and we will only use the Thomas-Fermi profiles to provide reasonable initial conditions, we will stick to it for simplicity (we have checked that the precise form of the initial functions is not crucial, see section III-B). In particular, we assume the initial profiles are Gaussian:

$$\psi_1|_{\tau=0} = \frac{\pi^{-\frac{1}{4}}}{\sqrt{w_{1,0}}}e^{\frac{-\eta^2}{2w_{1,0}^2}}, \quad \psi_2|_{\tau=0} = \sqrt{\frac{N_2}{N_1}}\frac{\pi^{-\frac{1}{4}}}{\sqrt{w_{2,0}}}e^{\frac{-\eta^2}{2w_{2,0}^2}} \qquad (9)$$

and determine $w_{1,0}$, $w_{2,0}$ by minimising the functional $E_{TF} = \int_{-\infty}^{\infty}\mathcal{E}_{TF}d\eta$ where:

$$\mathcal{E}_{TF} = f\,(|\psi_1|^2+|\psi_2|^2) + \frac{g_{11}}{2}|\psi_1|^4 + \frac{g_{22}}{2}|\psi_2|^4 + g_{12}|\psi_1|^2|\psi_2|^2 \qquad (10)$$

In the simplest, symmetric case $N_1 = N_2$, $g_{11} = g_{22} \equiv g = -g_{12} + \tilde{L}\sqrt{\pi}\tilde{V}_0$, one finds $w_{1,0} = w_{2,0} = \tilde{L}$. Evidently, the g_{ij} entering Eq. (10) are the values before the beginning of the manipulations, *i.e.* in the ground state of the trapped atoms.

The regime of validity of the GPE and its 1-D reduction has been widely discussed in the literature, see for instance [17, 33] and references therein. The dynamics is confined to one dimension if the interaction energy is not enough to excite higher modes in the transverse harmonic oscillator. In terms of adimensional quantities, this means, roughly $\sum_j |g_{ij}||\psi_j|^2 < 1$ for $i = 1, 2$ In all examples below, we will require this condition to hold at the center of the trap for the initial profiles. Thermal corrections of the GPE, which can eventually affect the evolution of the atom densities [34] or the coherence properties of the wavefunctions [35], will be disregarded in the analysis. It is also worth mentioning that large scattering lengths come together with high 3-body recombination rates which result in the depletion of the condensate — this, in fact, is the basis of a usual procedure for experimentally determining Feshbach resonances. However, the protocols that will be discussed in the following do not need extreme values of a_{ij} and we will not take this phenomenon into account.

In the following, with the aim of keeping some generality, the dimensionless notation is used in most of the equations. Figures will present examples with dimensionful values of the parameters. The translation between both formalisms is straightforward using the definitions given in this section. For instance, a typical value for $\omega_{1\perp}$ may be $10^3 \mathrm{s}^{-1}$. Then, if one considers ^{7}Li atoms, $r_\perp \approx 3\mu m$. With this in mind, one can get a ballpark estimate of the physical meaning of the dimensionless parameters: the unit of τ would correspond to 1 ms and the unit of η to $3\mu m$. Many examples are provided by choosing the different scattering lengths in order to have figures which illustrate neatly the general ideas. Notwithstanding, sections III-C, IV-B, V-A introduce cases using values of the scattering lengths and magnetic Feshbach resonances reported in the experimental literature for concrete atomic mixtures.

III. SOLITON EMISSION WITH A TIME-DEPENDENT INTERSPECIES SCATTERING LENGTH

The most obvious phenomenon that is present in multicomponent BECs but not in single species ones is that of inter-species forces. We will thus start our analysis by showing how by tuning this parameter it is possible to out-couple vector bright-bright solitons from a sample initially trapped in a shallow potential. Due to the large space of parameters there is a plethora of possibilities but, in order to focus in the desired dynamics, we will consider that only g_{12} varies in time.

As the simplest example, let us consider $\kappa = 1$, $N_1 = N_2$, $g_{11} = g_{22} \equiv g$ and, for $\tau < 0$ let us take $g_{12} = 0$. Thus, initially, the atom clouds for both species are identical and are well approximated by the Thomas-Fermi profile:

$$\psi_1 = \psi_2 = \frac{1}{\pi^{\frac{1}{4}}\sqrt{\tilde{L}}} \exp\left(-\frac{\eta^2}{2\tilde{L}^2}\right) \tag{11}$$

if we assume that $g = \sqrt{\pi}\tilde{V}_0\tilde{L}$. Notice that an initial relative phase would play no rôle in the evolution. By turning on $g_{12} = \tilde{g}_{12} > 0$ in the time interval $0 < \tau < \tau_s$, the cloud expands out of the trap due to the repulsive forces. Then, at a given time τ_s, one can tune $g_{12} = \hat{g}_{12} < -g < 0$ in order to spark modulational instability and vector soliton formation. The value of τ_s has to be chosen properly. If it is too small, repulsion would not be enough for the solitons to leave the trap. If it is too large, the cloud gets to disperse before tuning to $g_{12} < 0$ and soliton formation is impeded. See section III-A for a related discussion.

Due to the symmetry between both species in this simplified case, it is clear that the condition $\psi_1 = \psi_2$ can be a solution for the whole evolution and thus, formally, the system of equations is reduced to that of [13]. One could wonder whether this $\psi_1 = \psi_2$ solution is stable. In fact, that is the case for the soliton emission process. We will come back to this question in section III-B. Adapting the results of [13], a rough estimate to how the number of vector solitons emitted varies with the different quantities can be given:

$$N_s \approx 2\left[\frac{c_1\sqrt{-(g+\hat{g}_{12})}(c_2\sqrt{\tilde{g}_{12}+g} - \tilde{L})}{(\tilde{g}_{12}+g)^{\frac{1}{4}}}\right] \tag{12}$$

where c_1, c_2 can be fitted to data. The term $(c_2\sqrt{\tilde{g}_{12}+g} - \tilde{L})$ becomes negative for small g_{ij}, what might seem surprising. The point is that, since the solitons feel the Gaussian trap, they need a sufficient initial boost to be able to escape from it. Distinctly, the boost is provided by the repulsive interactions in the expansion period. If this repulsion is not large enough, the estimated N_s becomes negative, meaning that solitons, even if produced, are not able to overcome the trapping potential.

Let us now turn to a non-symmetric case $\kappa \neq 1$. The Thomas-Fermi initial profiles will be the same as before, but the subsequent evolution differs since it cannot be reduced to a single second order equation any more. Before showing the results of some characteristic simulations, we provide some analytic insight of the problem. The first step of the process is the expansion of the cloud due to repulsive $\tilde{g}_{12}$. A simple modelization can be constructed in the averaged Lagrangian formalism [36]. A variational ansatz is considered:

$$\psi_j = A_j(\tau)e^{\frac{-\eta^2}{2w_j(\tau)^2}}e^{i(\mu_j(\tau)+\eta^2\beta_j(\tau))} \tag{13}$$

Notice that the ansatz for the initial conditions was taken consistent with this form. These expressions are inserted into $\bar{\mathcal{L}} = \int_{-\infty}^{\infty} \mathcal{L} d\eta$ where:

$$\mathcal{L} = \sum_{j=1}^{2} \left[-\frac{i}{2}(\psi_j \partial_\tau \psi_j^* - \psi_j^* \partial_\tau \psi_j) + \frac{1}{2}|\partial_\eta \psi_j|^2 + \mathcal{E}_{TF} \right] \tag{14}$$

where $\mathcal{E}_{TF}$ can be found in Eq. (10). From the averaged Lagrangian $\bar{\mathcal{L}}$ one can write the Euler-Lagrange equations for the eight real fields $A_j(\tau), w_j(\tau), \mu_j(\tau), \beta_j(\tau)$. Since the main interest is to compute the evolution of the sizes of the clouds $w_j(\tau)$, we just write down the relevant equations:

$$\ddot{w}_1(\tau) = \frac{1}{w_1(\tau)^3} - \frac{2\tilde{L}\,\tilde{V}_0 w_1(\tau)}{(\tilde{L}^2 + w_1(\tau)^2)^{\frac{3}{2}}} + \\ + \frac{g_{11}}{\sqrt{2\pi}\, w_1(\tau)^2} + \frac{N_2^2}{N_1^2} \frac{2 g_{12} w_1(\tau)}{\sqrt{\pi}(w_1(\tau)^2 + w_2(\tau)^2)^{\frac{3}{2}}}\,. \tag{15}$$

$$\ddot{w}_2(\tau) = \frac{\kappa^2}{w_2(\tau)^3} - \frac{2\kappa\,\tilde{L}\,\tilde{V}_0 w_2(\tau)}{(\tilde{L}^2 + w_2(\tau)^2)^{\frac{3}{2}}} + \\ + \frac{N_2^2}{N_1^2} \frac{g_{22}}{\sqrt{2\pi}\, w_2(\tau)^2} + \frac{2\kappa\, g_{12} w_2(\tau)}{\sqrt{\pi}(w_1(\tau)^2 + w_2(\tau)^2)^{\frac{3}{2}}}\,. \tag{16}$$

This suggests that, if the expansion is driven by the interspecies repulsion g_{12}, and assuming $N_1 \approx N_2$, the less massive cloud of atoms expands faster. The simulation of figure 1 confirms this expectation. Taking $\kappa = 0.3061$, as it corresponds to a lithium-sodium mixture, the simulation was performed with the dimensionless parameters $g_{11} = g_{22} = 1$, $N_1 = N_2 = 50000$, $\tilde{V}_0 = 1/15$, $\tilde{L} = 15$ and $\tilde{g}_{12} = 15$. These quantities have been introduced fixing $\omega_\perp = \omega_{1\perp,2\perp} = 10^3 \mathrm{s}^{-1}$, and the rest of dimensional parameters presented in the caption. The figure also shows how bumps appear in the wave-functions even in the absence of attractive interaction. Notice these bumps do not have a solitonic character and tend to spread out.

The second step of the process is soliton formation after tuning g_{12} to a negative value therefore sparking modulational instability. We show the result of numerical simulations in figure 2. As a representative example we have taken again a lithium-sodium mixture, that is $\kappa = 0.3061$, and the dimensionless parameters $g_{11} = g_{22} = 1$, $N_1 = N_2 = 50000$, $\tilde{V}_0 = 1/15$, $\tilde{L} = 15$, $\tau_s = 25$, $\tilde{g}_{12} = 15$ before τ_s and $\hat{g}_{12} = -6$ after τ_s. These quantities were introduced fixing $\omega_\perp = \omega_{1\perp,2\perp} = 10^3 \mathrm{s}^{-1}$ and their correspondent dimensional parameters are presented in the caption of the figure. It can be observed how the repulsive interspecies force pushes part of the atomic cloud out of the trap, with the lighter atoms in front. The sudden change of g_{12} leads to the grouping of a bunch of atoms. Even if the process is not symmetric under the change $\psi_1 \leftrightarrow \psi_2$, the attractive interactions eventually groups a fraction of the atoms into vector solitons which escape from the trap thanks to their own inertia. In this case, a single soliton pair is produced.

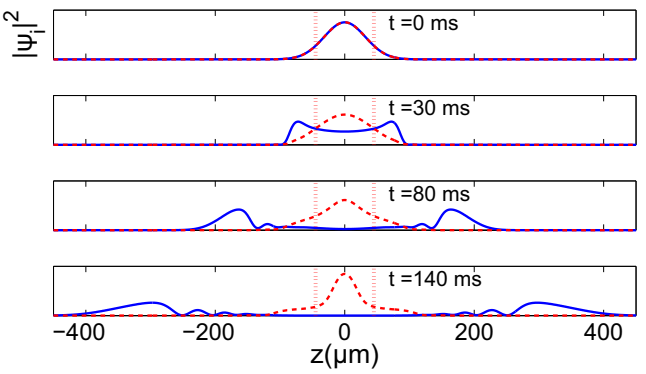

FIG. 1: (Color online). An example of evolution in time of the atom densities of both species $|\psi_1|^2(z)$ (solid blue line) for lithium, $|\psi_2|^2(z)$ (red dashed line) for sodium. These simulation have been performed with parameters $a_{11} = a_{22} = 0.3nm$, $N_1 = N_2 = 50000$, $V_0 = \hbar\omega_\perp/15$, $L = 45\mu m$. The inter-species scattering length parameter is tuned from $a_{12} = 0$ to $\tilde{a}_{12} = 0.45nm$. The red dashed vertical lines located at $z = \pm L$ indicate the size of the shallow trap.

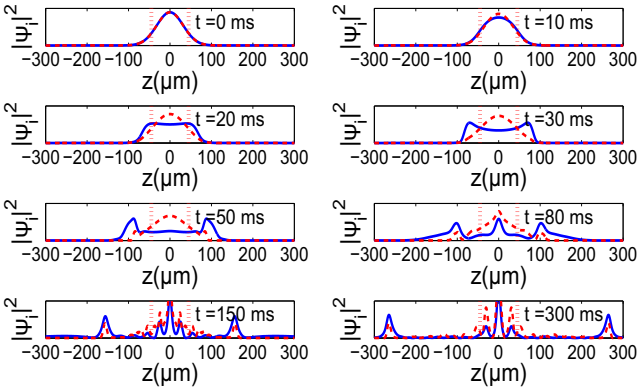

FIG. 2: (Color online). Simulation with parameters $\kappa = 0.3061$, $a_{11} = a_{22} = 0.3nm$, $N_1 = N_2 = 50000$, $V_0 = \hbar\omega_\perp/15$, $L = 45\mu m$. Taking $t_s = 25ms$, the inter-species scattering length parameter is tuned from $a_{12} = 0$ for $t < 0$ to $\tilde{a}_{12} = 0.45nm$ for $0 < t < t_s$ to $\hat{a}_{12} = -0.18nm$ for $t > t_s$. The solid blue line corresponds to lithium and the dashed red line to sodium.

In the asymmetric case $\kappa \neq 1$, it does not seem possible to provide a simple reliable formula which estimates the number of emitted solitons, similar to Eq. (12). However, some qualitative features remain: below a certain value of $\tilde{g}_{12}$, the repulsive force is not strong enough and no vector soliton comes out. Then, the number of solitons grows with increasing $\tilde{g}_{12}$ since more atoms are outcoupled from the trap. These features can be easily appreciated in figure 3, which shows the results of a sample of simulations. The figure also shows that the number of emitted solitons slightly decreases with κ. The dependence on $\hat{g}_{12}$ is weaker: as long as this attraction is large enough to pack the out-coming atoms into vector solitons, it hardly affects its number.

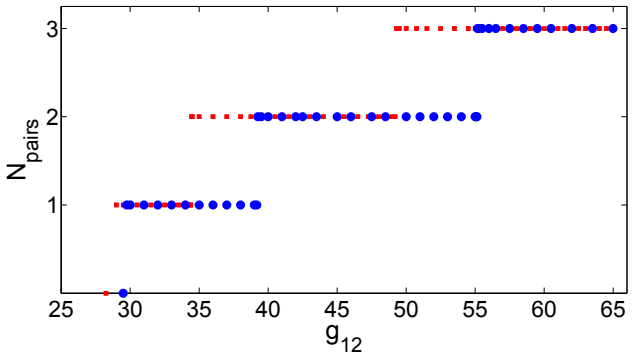

FIG. 3: (Color online). Number of out-coupled vector soliton pairs vs. the inter-species scattering length driving the expansion $\tilde{g}_{12}$. Blue circles correspond to $\kappa = 0.31$ (a lithium-sodium mixture) and red squares to $\kappa = 0.47$ (a potassium-rubidium mixture). The rest of parameters are fixed as in figure 2. The conversion to a_{12} can be made using Eq. (6), taking $\omega_\perp = 10^3 \mathrm{s}^{-1}$ and $r_\perp \approx 3\mu m$ (for the lithium-sodium mixture) or $r_\perp \approx 1.25\mu m$ (for the potassium-rubidium mixture).

A. Possible limitations in the time of tuning

The method of soliton emission presented in this paper has considered, until now, instant modifications in the inter-species scattering length. This is an ideal assumption, since such a sudden tuning from zero to the chosen value is impossible. Consequently, it is important to analyse what happens when this parameter is changed in a smoother way. In the following, different simulations are presented in order to check the possible time limitations in the a_{12} tuning to get the right initial triggering and soliton outcoupling processes. The parameters will be those displayed in figure 2 with the only difference that a_{12} is now defined by:

$$a_{12} = \begin{cases} 0 & \text{if } t \leq 0 \\ \frac{\tilde{a}_{12}}{t_1} t & \text{if } 0 < t < t_1 \\ \tilde{a}_{12} & \text{if } t_1 \leq t \leq t_2 \\ \frac{\hat{a}_{12}(t-t_2) - \tilde{a}_{12}(t-t_3)}{t_3 - t_2} & \text{if } t_2 < t < t_3 \\ \hat{a}_{12} & \text{if } t \geq t_3 \end{cases} \qquad (17)$$

where the different time instants t_1, t_2 and t_3 were introduced in order to modify a_{12} gradually until reaching its maximum and minimum values $\tilde{a}_{12}$ and $\hat{a}_{12}$. The quantities $\Delta t_1 = t_1 - 0 = t_1$ and $\Delta t_2 = t_3 - t_2$ represent respectively how fast each tuning is and they are the subject of study.

Let us start with the analysis of the tuning for the expansion, that is in $0 \leq t \leq t_2$. It turns out that the important factor is the kinetic energy acquired by the atom cloud during its expansion. If the expansion rate is not enough, solitons collapse re-entering the trap, see Fig. 4.

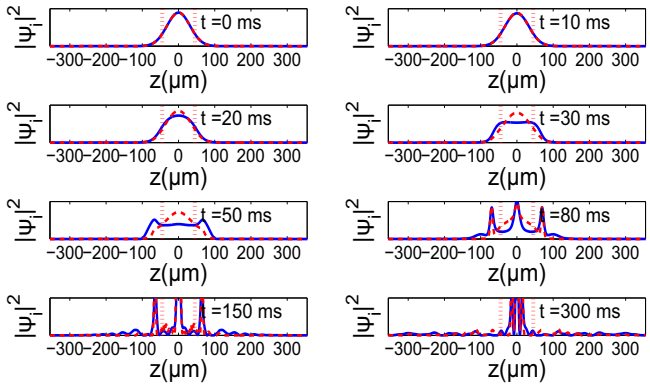

FIG. 4: (Color online). Simulation with the same parameters that in figure 2 except for a_{12}. The following values have been taken: $t_1 = 19ms$, $t_2 = 25ms$ and $t_3 = 27ms$, so $\Delta t_1 = 19ms$ and $\Delta t_2 = 2ms$. The solid blue line corresponds to lithium and the dashed red line to sodium.

The conclusion is that the time Δt_1 is not decisive as it can be always compensated by delaying t_2, see Fig. 5 where soliton emission is similar to that in Fig. 2.

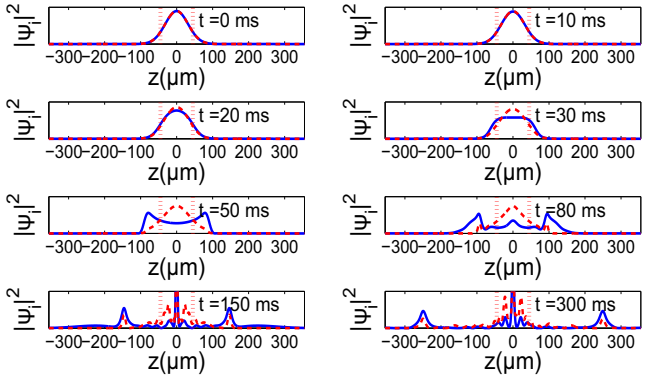

FIG. 5: (Color online). Simulation with parameters $t_1 = 26ms$ — so $\Delta t_1 = 26ms$ — and $t_2 = 38ms$, $t_3 = 40ms$ — so $\Delta t_2 = 2ms$. The rest of parameters are the same that in figure 2. The solid blue line corresponds to lithium and the dashed red line to sodium.

Let us turn to the tuning involved in the soliton formation, that is in $t > t_2$. Our simulations show that there is a limiting value for Δt_2 above which solitons are not produced. The reason is that the atom cloud spreads out excessively before the self-trapped atom clusters are actually formed. Fig. 6 provides an example of this fact.

The specific constraint on Δt_2 depends non-trivially on all the rest of parameters, but, roughly, a few miliseconds seem enough to get success in soliton formation.

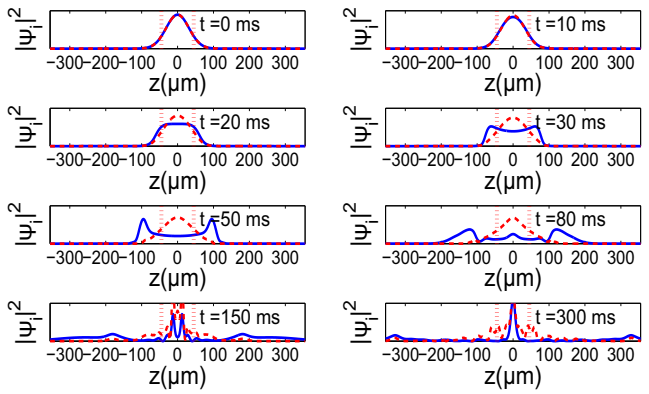

FIG. 6: (Color online). Simulation with the same parameters that in figure 2 except for a_{12}. In these plots, $t_1 = 5ms$, $t_2 = 25ms$ and $t_3 = 45ms$, so $\Delta t_1 = 5ms$ and $\Delta t_2 = 20ms$. The solid blue line corresponds to lithium and the dashed red line to sodium.

B. Introduction of noise in the process

Another relevant question is how robust the results described are. For instance, in the symmetric $\kappa = 1$, $N_1 = N_2$ case, it is not obvious whether the evolution with $\psi_1 = \psi_2$ locked to each other is stable. Indeed, in a situation without potential and flat atomic distributions, the system is modulationally unstable even if all interactions are repulsive as long as $g_{12}^2 > g_{11}g_{22}$. However, it can be checked with simulations that, in the processes described, the outcome is well described by the $\psi_1 = \psi_2$ solution. What happens is that when the solitons are formed, the differences that had appeared during the expansion of the cloud are partially washed out. As an illustration, we depict in figure 7 a comparison of the result of simulations with and without random noise introduced in the initial conditions. The noise was introduced by multiplying the discrete Fourier transform of the initial Gaussian profiles by real pseudo-random numbers extracted from a normal distribution with mean 1 and standard deviation 0.2. After this random modification, the wave-functions are normalized by dividing by a global factor. It can be appreciated how the out-coupled vector soliton pair is almost unaffected by the noise.

With this kind of simulations, it can also be checked that the precise form of the initial profile is not a critical factor for the qualitative evolution of the atom cloud. For this reason, using Thomas-Fermi in order to insert the initial conditions is a justified approximation.

C. Experimental considerations

Even if the rich structure of Feshbach resonances in different mixtures of alkali atoms results in an ample set of possibilities for manipulation, it is clear that not all

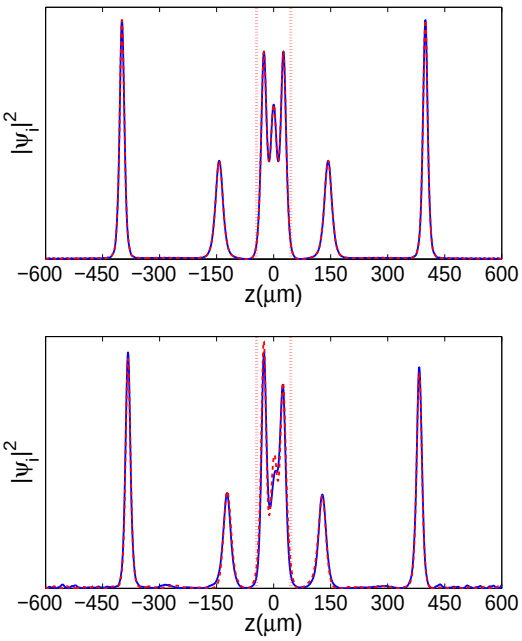

FIG. 7: (Color online). Emission of a vector soliton pair in the symmetric case. All parameters are as in figure 2 except for $\kappa = 1$. Above, a noise-less simulation where the result has strictly $\psi_1 = \psi_2$. Below, random noise was introduced in the initial conditions.

protocols that one may imagine can be realized in the laboratory. Around a magnetically tuned Feshbach resonance, the scattering length varies as [16]:

$$a(B) = a_{bg}\left(1 - \frac{\Delta}{B - B_0}\right) \tag{18}$$

where B_0 is the position of the resonance, Δ its width and a_{bg} the off-resonance value of the s-wave scattering length. In a two-component mixture, similar expressions hold for each intra-species interaction and for the inter-species one. Thus, the three relevant scattering lengths depend on a single externally tunable parameter B.

The implementation of the process described in this section requires the possibility of widely tuning a_{12} while a_{11}, a_{22} remain positive and essentially constant. Understanding which are all the mixtures in which this is possible lies beyond the scope of the present work, but we now argue that in ^{7}Li-^{23}Na it can be accomplished, at least in principle.

For sodium, the background value away from a few narrow resonances is $a_{22} \approx 63a_0$ where $a_0 \approx 0.053nm$ is Bohr radius — see [16] and references therein. ^{7}Li in its $|F = 1\ m_f = 1\rangle$ hyperfine state presents a broad resonance with $B_0 \approx 736.8$G, $\Delta \approx -192.3$G and $a_{bg} \approx -25a_0$ [3, 37]. It is worth mentioning that this was the isotope used in the first experiments showing the formation of bright (single-species) solitons [3, 4]. In the region between the zero-crossing point $B_{zc} \approx 544$G and the reso-

nance, the scattering length remains positive and varies according to Eq. (18), as experimentally studied in detail in [37]. Several inter-species ^{7}Li-^{23}Na resonances were predicted in [38] fitting experimental observations for ^{6}Li-^{23}Na to a theoretical coupled-channel model. In particular, there are two of them around $B_0 \approx 600$G and $B_0 \approx 650$G. We conclude that by tuning the magnetic field around these values, a_{12} can be drastically shifted while a_{22} does not change and a_{11} varies only mildly, providing a possible experimental scenario in which to realize the suggested out-coupling of vector solitons.

Figure 8 shows the process of soliton emission for this case. The widths of the initial Gaussian profiles $w_{1,0}$ and $w_{2,0}$ were calculated for this simulation minimising Eq. (10). It can be observed that the outcome is qualitatively simliar to Fig. 2 despite notorious differences in some of the parameters entering the computation.

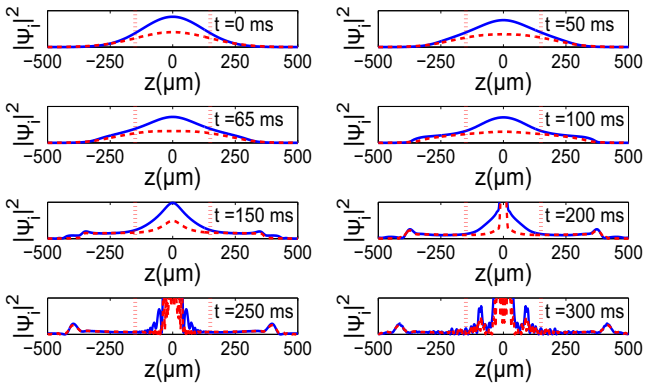

FIG. 8: (Color online). Simulation with parameters $\kappa = 0.3061$, $a_{11} = 30a_0$, $a_{22} = 63a_0$, $N_1 = 50000$, $N_2 = 30000$, $V_0 = 0.5\hbar\omega_\perp$, $L = 150\mu m$. Taking $t_s = 65ms$, the inter-species scattering length parameter is tuned from $a_{12} = 0$ for $t < 0$ to $\tilde{a}_{12} = 3.3nm$ for $0 < t < t_s$ to $\hat{a}_{12} = -2.25nm$ for $t > t_s$. The solid blue line corresponds to lithium and the dashed red line to sodium.

IV. EXTRACTING MATTER WITH MATTER

In this section we will focus on the possibility of using one species in order to control the atom cloud of the second one through the inter-species force. This indirect manipulation can be specially useful when it is simpler to manipulate one of the components of the mixture. We will show that in this fashion it is possible to out-couple trapped matter waves if the inter-atomic attraction is strong enough. Notice that the idea is similar to the one underlying the technique that allowed to create the first mixed BECs [39], where one of the species was cooled down whereas the temperature of the second one only decreased by interaction with the first.

The simplest way to realize control of the species 2 via species 1 is to consider $N_1 \gg N_2$. In the limit $N_2/N_1 \to 0$, the computation can be split in a two step process. First, one has to solve a non-linear equation for ψ_1 in which the second species can be ignored. Then, assuming that the self-interaction of the second species is negligible, one can solve the *linear* Schrödinger equation for the second species in which the total potential is given by the sum of the external potential and the effective, time dependent, potential induced by the atom cloud of the first species, namely:

$$f_{2,tot} = f_2 + g_{12}|\psi_1|^2 \tag{19}$$

On the other hand, when the second species back-reacts on the first one, the coupled system of equations must be solved. Two different situations in which these general ideas may be realized will be considered in turn.

A. A soliton extracts matter from a trap

Let us consider species 2 as starting in the ground state of the linear Schrödinger equation with trapping potential (8). The values $\tilde{V}_0 = 1/15$, $\tilde{L} = 15$ will be fixed. The ground state wave-function can be easily computed by a numerical shooting method. We then compute its evolution when a bright soliton of species 1 traverses the atom cloud with velocity v. We take $g_{11}, g_{12} < 0$ and:

$$|\psi_1|^2 = -\frac{g_{11}}{4}\frac{1}{\cosh^2(-\frac{g_{11}}{2}(\eta - (\eta_0 + v\,\tau)))} \tag{20}$$

By inserting this expression into (19), (4), it is possible to study what happens to species 2 for different values of g_{11}, g_{12}, v. In order to understand the results, we start by writing down the following Schrödinger equation:

$$-\frac{1}{2}\frac{\partial^2\psi_2}{\partial x^2} - \frac{s(s+1)}{2\cosh^2 x}\psi_2 = E\,\psi_2 \tag{21}$$

which, after some redefinitions, including:

$$\frac{g_{12}}{g_{11}} \equiv \frac{s(s+1)}{2} \tag{22}$$

can be found to be the equation governing the second species in the presence of a static soliton of the first one. In fact, the $s = 1$ case, corresponding to $g_{11} = g_{12}$ is called the one-soliton potential, see for instance [40]. For $s > 0$, the discrete spectrum consists of $\lceil s \rceil$ eigenstates of energies $-(s-n)^2/2$ with $n = 0, 1, \ldots, \lceil s \rceil - 1$, see [41]. The continuous spectrum of (21) is remarkable since the potential proves to be reflection-less if s is an integer [42].

This last observation is important for the problem at hand since, for $|g_{11}| \gtrsim 1$, it can be observed that if $\frac{g_{12}}{g_{11}} = 1, 3, 6, 10, \ldots$, the soliton passes through the trap almost without affecting it, so the soliton continuous its path and it does not practically extract atoms of the cloud. On the other hand, for other values of $\frac{g_{12}}{g_{11}}$ — non-integer s —, the

potential in (21) ceases to be reflection-less and, indeed, the passing soliton pushes atoms out of the trap. Both behaviours can be discerned in Fig. 9. The simulations where performed with the dimensionless parameters $\eta_0 = -50$ and $v = 0.2$ for the two plots, taking $g_{11} = -2$, $g_{12} = -6$ on the left plot and $g_{11} = -2$, $g_{12} = -6$ on the right one. Considering a number of 5000 atoms per soliton and atoms of ^{7}Li, so that $r_\perp \approx 3\mu$m, the correspondent dimensionful parameters are presented in the caption of the figure. On the right plot, the atoms of the second species exit the trap in front of the soliton, as a tennis ball hit by a racket, so these atoms are not a solitonic wave. For fixed g_{12}/g_{11} and v, the number of out-coupled atoms grows with $|g_{12}|, |g_{11}|$ since the interaction is stronger.

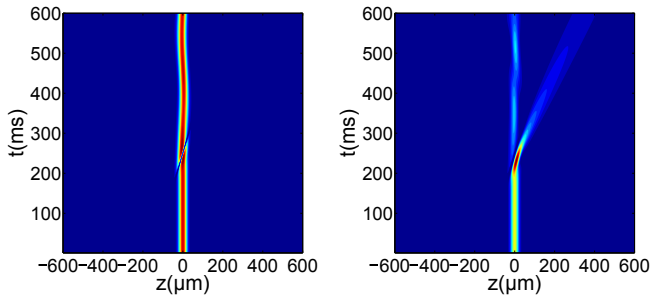

FIG. 9: (Color online). Contour plots of the time evolution of the wave-function $|\psi_2|^2$. In both cases $z_0 = -150\mu m$, $v = 0.6\mu m/ms$. On the left, $a_{11} = -0.6nm$, $a_{12} = -1.8nm$. On the right, $a_{11} = -0.6nm$, $a_{12} = -1.2nm$.

The situation changes for small g_{11}, when the soliton size is comparable to the trap size, Fig. 10 — a situation which may be difficult to achieve experimentally but which we believe is worth discussing. The dimensionless parameters of the simulations were $\eta_0 = -50$ and $v = 0.2$ for the two plots, taking $g_{11} = -0.5$, $g_{12} = -0.5$ on the left plot and $g_{11} = -0.5$, $g_{12} = -1.5$ on the right one. The dimensional parameters in the caption of the figure were calculated using the same considerations as for Fig. 9. In Fig. 10, it turns out that the soliton captures part of the cloud of the second species, which comes out of the trap in one of the discrete eigenstates of (21) (appropriately Galileo-transformed to have the same velocity as the soliton).

In summary, there are three types of qualitative behaviour. The soliton can traverse the trap leaving it undistorted (fig 9a), it can push atoms out of the trap without capturing them so the outcoupled atoms form a dispersive wave (fig 9b) or it can capture atoms of the second species so the outcome is a vector soliton (fig 10).

It is also interesting to discuss the dependence on v of the number of extracted atoms. The precise behaviour depends on the parameters g_{11}, g_{12} but, in general, the fraction of out-coupled atoms has a maximum at a certain velocity and then decreases for larger velocities, as it could be expected since reflection from a potential

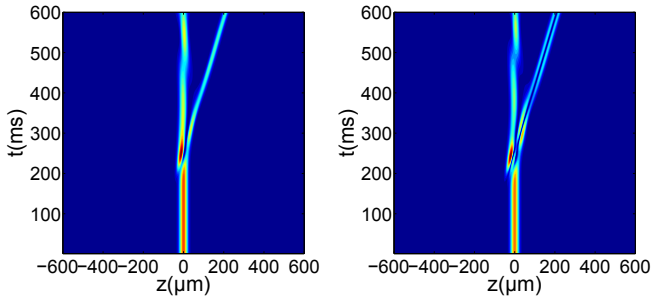

FIG. 10: (Color online). Contour plots of the time evolution of the wave-function $|\psi_2|^2$. In both cases $z_0 = -150\mu m$, $v = 0.6\mu m/ms$. On the left, $a_{11} = -0.15nm$, $a_{12} = -0.15nm$. On the right, $a_{11} = -0.15nm$, $a_{12} = -0.45nm$; it can be observed how the second species is extracted in the first excited state of the potential in Eq. (21).

is typically smaller for larger momentum. Nevertheless, for small values of $|g_{11}|$ there are more complicated behaviours. The wave-function $|\psi_2|^2$ starts oscillating around the moving soliton inside the trap. For some particular values of v, it coincides that the soliton exits the trap while the oscillation of the cloud around it moves rightwards. This sort of resonance enhances the atom out-coupling. An example is shown in Fig. 11, where more than 90% of the atoms are extracted from the trap. The simulation was performed with the dimensionless parameters $\eta_0 = -50$, $v = 0.2$, $g_{11} = -0.25$ and $g_{12} = -2.8$. The dimensionful parameters are presented again attending to the considerations exposed in Fig. 9.

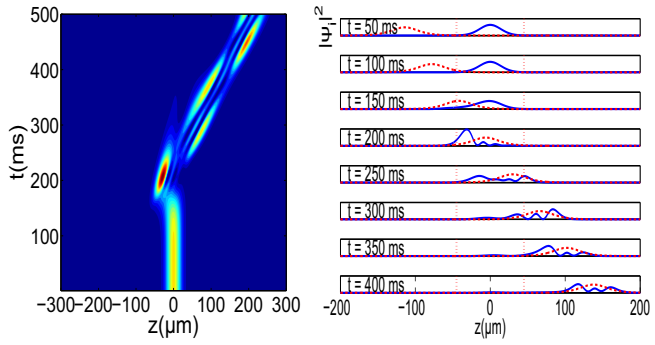

FIG. 11: (Color online). Almost complete extraction $a_{11} = -0.075nm$, $a_{12} = -0.84nm$, $v = 0.72\mu m/ms$.

In Fig. 12, some data obtained from the numerical simulations which condense the discussion of this section are presented. The fraction of out-coupled atoms are represented in terms of the different dimensionless parameters. Again, the dimensionful parameters are calculated as in the previous figures.

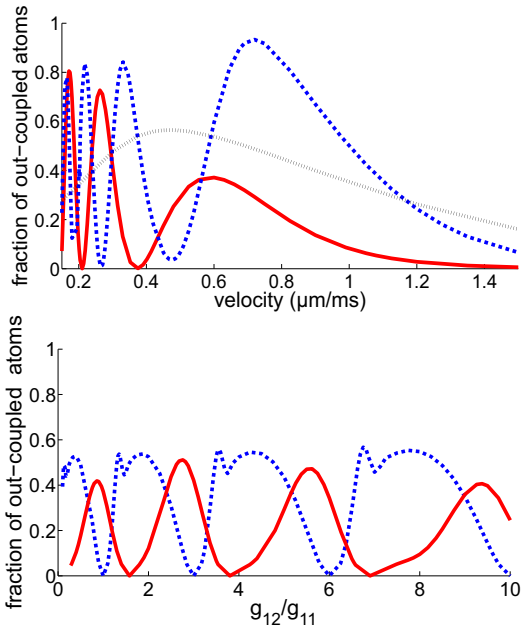

FIG. 12: (Color online). Fraction of out-coupled atoms. Top: as a function of velocity. The three graphs correspond to $g_{11} = -0.5$ ($a_{11} = -0.15nm$), $g_{12} = -0.5$ ($a_{12} = -0.15nm$) for the solid red line; $g_{11} = -0.25$ ($a_{11} = -0.075nm$), $g_{12} = -2.8$ ($a_{12} = -0.84nm$) for the dashed blue line; $g_{11} = -2$ ($a_{11} = -0.075nm$), $g_{12} = -3.7$ ($a_{12} = -1.11nm$) for the dotted black line. Bottom: as a function of g_{12}/g_{11}. The two graphs correspond to $g_{11} = -2$ ($a_{11} = -0.6nm$), $v = 0.2$ ($v = 0.6\mu$m/ms) for the dashed blue line; $g_{11} = -0.5$ ($a_{11} = -0.15nm$), $v = 0.2$ ($v = 0.6\mu m/ms$) for the solid red line.

B. Both species are initially trapped

Now we start with the two species confined in the trap with the idea of controlling species 2 with the first one. The evolution of the first species is driven by modifying in time its correspondent intra-species parameter a_{11} to produce solitons by modulational instability, along the lines of [13]. If $N_2 \ll N_1$, the presence of the other species affects this process only mildly. If the interspecies force is attractive, these out-coupled solitons can capture matter from the second species, with the possibility of forming vector solitons. Indeed, with $a_{12} < 0$, the first species generates "local traps" where the atoms of the second species tend to fall.

It is also important that the initial Gaussian profile for the second atom cloud $w_{2,0}$ is wider than that of the first one $w_{1,0}$. The reason is that, when the solitons are formed in the first species, they cannot be very far of the atoms of the second species, or otherwise they would hardly trap them. Thus, for the $t < 0$ situation, one needs $a_{22} > 0$ such that $a_{22} > a_{11}$. For given a_{ij} , both values of the Gaussian width profiles, $w_{1,0}$ and $w_{2,0}$, can be determined minimising the functional E_{TF} of section II, see Eq. (10).

A concrete example is furnished by considering a ^{7}Li-^{87}Rb mixture in their lower hyperfine states. There are a broad intraspecies resonance for lithium [3, 37] and a broad interspecies resonance [43] such that:

$$a_{11} = -25a_0\left(1 + \frac{192.3}{B - 736.8}\right)$$
$$a_{12} = -36a_0\left(1 + \frac{70}{B - 649}\right) \quad (23)$$

where B is the external magnetic field in Gauss. For ^{87}Rb, the background value will be fixed $a_{22} = 100a_0$ [16]. The mass ratio is $\kappa = 0.081$ and we take $N_1 = 5 \times 10^4$, $N_2 = N_1/10$. As in previous section, $\omega_{1\perp} = \omega_{2\perp} = 10^{-3}$s such that $r_\perp = 3\mu$m. The parameters of the trap will be taken to be $\tilde{L} = 30$ (namely $L = 90\mu$m) and $\tilde{V}_0 = 0.18$. Initially, the magnetic field is set to be $B = 579$G ($a_{11} = 0.29$nm, $a_{12} = 0$) and the initial atom distributions have $w_1 = \tilde{L}$, $w_2 = 1.73\tilde{L}$. At $t = 0$, the magnetic field is switched to $B = 697$G ($a_{11} = 5.1$nm, $a_{12} = -4.7$nm) and the stretching of the cloud commences. At $t = 8$ms, the field is switched off $B = 0$ ($a_{11} = -1$nm, $a_{12} = -1.7$nm) in order to initiate soliton formation. The result is shown in figure 13. As expected, the evolution of ^{7}Li is essentially unaffected by the less numerous rubidium atoms and the corresponding plot is similar to those found in [13]. On the right plot, it can be observed how a set of rubidium atoms are trapped by the lithium consequently forming a vector soliton. It can also be appreciated that there is a number of atoms of this second species which are out-coupled from the trap which are not packed in the soliton.

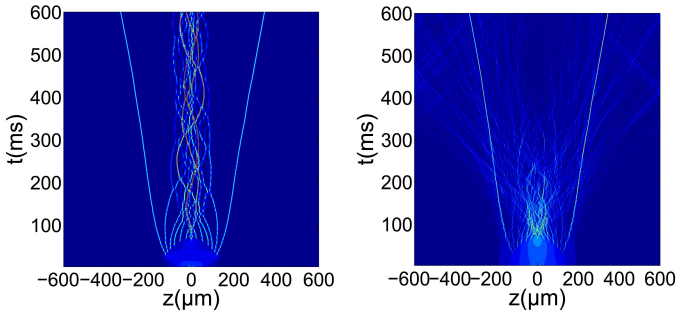

FIG. 13: (Color online). Emission of a pair of vector solitons with $N_1 \gg N_2$. On the left, the plot representing lithium; on the right, the rubidium. The parameters entering the simulation are presented in the text.

V. CREATING SUPERSOLITONS

When solitons of two different species with repulsive interactions between them form an alternating array, they can behave as solid spheres in a Newton's cradle-like set-up. Thus, a perturbation propagates along the array as

an undistorted wave, analogous to a phonon, which was dubbed *supersoliton* in [23]. Modulational instability was mentioned in [23] as the natural way of seeding such an alternating array. The goal of this section is to explicitly show how this can be accomplished by suitably manipulating in time the inter-atomic forces.

For concreteness, we fix $\kappa = 1$ and $g_{11} = g_{22} = g$, but it should be understood that these conditions are not essential for the qualitative features of the process. A slight asymmetry is introduced $N_2 = 0.95N_1$ in order to avoid that $\psi_1 = \psi_2$ is a solution, see section III. In any case, the supersoliton excitation could also be produced in a fully symmetric set-up since in this case the symmetric solution tends to be unstable during the whole process: in a situation with $g_{11} < 0$, $g_{22} < 0$, $g_{12} > 0$, modulational instability always sets in [27, 28]. The following protocol is considered: initially, all scattering lengths are repulsive, producing the stretching of the atom cloud. Then, the intraespecies scattering lengths are tuned to negative values producing the instability. Due to interspecies repulsion, the system can evolve into the desired alternating array of solitons, see Figure 14.

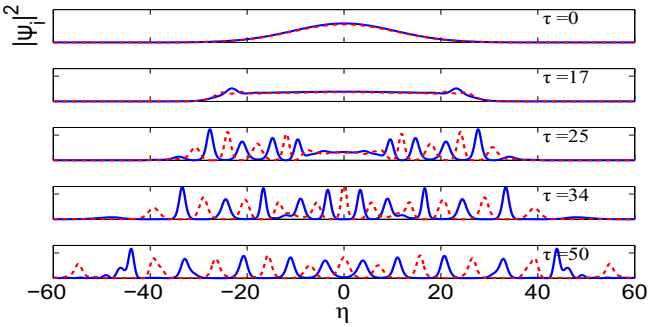

FIG. 14: (Color online). In this graph, $g = g_{12} = 15$ for $\tau < \tau_s = 10$ whereas $g = -20$ and $g_{12} = 15$ for $\tau > \tau_s$. The rest of parameters are $\kappa = 1$, $N_2 = 0.95N_1$

Once the alternating array is formed and in order to produce a kick, a potential wall can be placed in the way of the fastest soliton. The soliton bounces back to collide with the adjacent one therefore starting a supersoliton-like excitation in the sample, providing a simple realization of the ideas of [23]. In particular, it is illustrative to implement a time-dependent step-like potential:

$$f_s = f_{s,0}(\tanh(\eta-\eta_s)-\tanh(\eta+\eta_s)+2\tanh(\eta_s))\Theta(\tau_b-\tau) \quad (24)$$

where $\Theta(x)$ is Heaviside function and τ_b is the time of the bounce of the fastest soliton at the step. The expression in Eq. (24) has to be added to the Gaussian trap (8). Figure 15 shows how the solitons act as hard balls because of their strong inter-repulsion.

The number of atoms per soliton can be easily estimated by integrating $|\psi_i|^2$ in the relevant region. As expected, once the alternating array is formed, the number of atoms per soliton does not change upon latter time

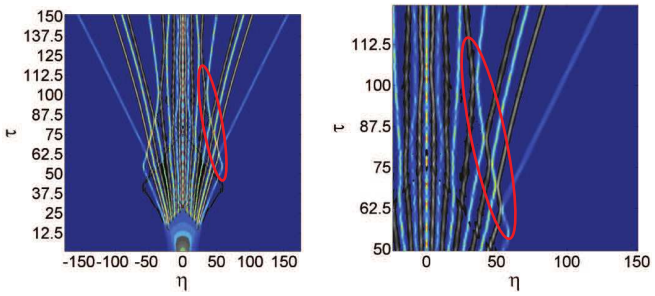

FIG. 15: (Color online). The left plot shows how the system acts like an array of hard balls colliding among themselves. On the right, the region of the supersoliton-like excitation is enlarged and indicated with a red ellipse.

evolution. This can be also checked in a non-symmetric case with $\kappa \neq 1$, where the qualitative behaviour is analogous to the above described.

A. Experimental feasibility

The described process requires a simultaneous tuning of both intra-species scattering lengths while the inter-species one remains fixed. For magnetically tuned Feshbach resonances — see Eq. (18) — approximately equal values of B_0 would be needed for both species. We are not aware of any mixture in which this coincidence happens and, in fact, it can be considered a marginal situation. An intriguing possibility would be to use optical methods [44] together with magnetic ones in order to independently displace the two closed channel levels and make the Feshbach resonances coincide. However, since we are not aware of any experimental result in this direction, we leave the previous discussion as a theoretical possibility and now look for situations in which similar processes can be achieved by tuning just one of the three relevant scattering lengths.

With this aim, let us consider a BEC composed by ^{7}Li and ^{23}Na, both in the hyperfine $|F = 1\ m_f = 1\rangle$ state. One can make use of the intra-species resonance around $B = 736.8$ G for ^{7}Li [37] which allows to tune the value of a_{11}. The other intra-species and the inter-species interaction would correspond to their background values $a_{22} \approx 63a_0$ [16] and $a_{12} \approx 20a_0$ [38].

Figure 16 shows the formation of the array for this case. It can be appreciated how species 1 forms solitons and the species 2 dispersive waves, since a_{22} is kept positive. Fixed $g_{22} = 67$ and $g_{12} = 22$, the taken dimensionless scattering lengths were $g_{11} = 155$ for $\tau < \tau_s = 40$ whereas $g_{11} = -35$ for $\tau > \tau_s$. The rest of parameters were $\kappa = 0.3061$, $\tilde{L} = 60$, $\tilde{V}_0 = 0.75$ and $N_1 = N_2 = 30000$. The correspondent dimensionful values are displayed in the caption of the figure.

Again, the potential wall of Eq. (24) is added to the

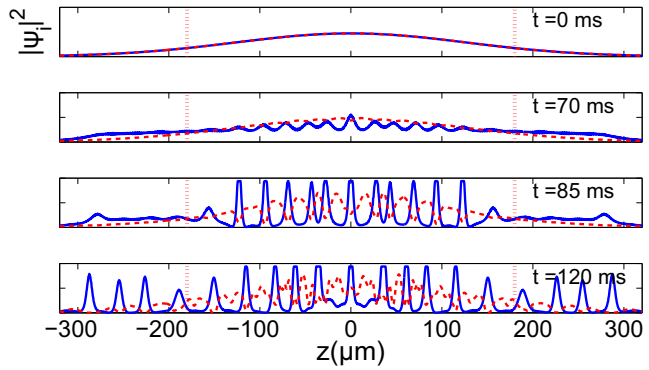

FIG. 16: (Color online). In this graph, $a_{11} = 7.75nm$, $a_{22} = 63a_0$ and $a_{12} = 20a_0$ for $t < t_s = 40ms$ whereas $a_{11} = -1.75nm$, $a_{22} = 63a_0$ and $a_{12} = 20a_0$ for $t > t_s$. The rest of parameters are $\kappa = 0.3061$, $L = 180\mu m$, $V_0 = 0.75\hbar\omega_\perp$, $N_1 = N_2 = 30000$.

Gaussian trap (8). In figure 17 the soliton of species 1 bounces back to collide with the matter waves of species 2, therefore sparking a pseudo-supersoliton excitation. Notice that species 2 plays a crucial role in the process even if its atoms are not packed in solitons themselves.

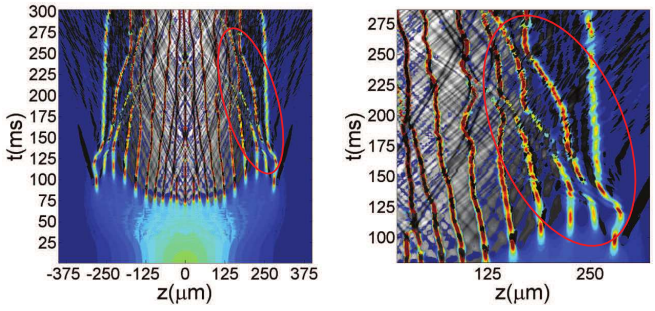

FIG. 17: (Color online). Example of pseudo-super-solitons colliding after the formation of the array in a mixture of ^{7}Li-^{23}Na. On the right, the region of the supersoliton-like excitation, which is indicated with a red ellipse, is enlarged.

Another mixture for which one can conceive a similar phenomenon is that composed by ^{85}Rb in its hyperfine $|F = 2\ m_f = -2\rangle$ state and ^{87}Rb with $|F = 1\ m_f = -1\rangle$ [45]. Near the intra-species resonance around $B = 155$ G for ^{85}Rb [46], it is possible to tune the value of a_{11}. This resonance has been crucial in the attainment of a BEC with only ^{85}Rb atoms [47], in the formation of bright soliton after its collapse [48] and in the achievement of the mentioned two-species condensate [45]. Around this value of the magnetic field, the other intra-species and the inter-species interaction are away from any resonance and correspond to their background values $a_{22} \approx 100a_0$ [49] and $a_{12} \approx 213a_0$ [50]. Nevertheless, an eventual experiment with this mixture may be more delicate because of the large value of a_{12}, which can induce modulational instability in the initial phase when all scattering lengths remain positive.

VI. DISCUSSION

The degree of control of cold atomic clouds that has been experimentally achieved is remarkable. In this contribution, we have theoretically discussed several possibilities of atom manipulation of two-component BECs trapped in quasi-one-dimensional potentials, by tuning in time the different inter-atomic forces. We have shown that there are several interesting phenomena that can occur in multicomponent systems and that do not have any obvious counterpart in the single species case. Having both inter- and intra-species scattering which can be separately tuned in time and/or space opens a plethora of possibilities of which we have explored a few. We emphasize that numerical simulations indicate that the qualitative behaviours shown are rather robust in the sense that they do not depend crucially on the shape of the trap, the initial profile or the particular atomic species for which the computations are done. They do depend, though, on the concrete values of the a_{ij} and the instants chosen for their tuning. Inappropriate values can result in a failure in the formation or the out-coupling of solitons. In any case, the essential point is the ability to externally control the interatomic forces in the desired ways.

Markedly, there are a number of different protocols that can be used in order to out-couple matter from shallow traps, providing atom laser-like devices. It can be of particular interest the possibility of using matter to manipulate matter as discussed in section IV since this could eventually lead to a sort of *atomic tweezers* that might generalize the laser tweezers which are readily used for atom manipulation, see for instance [51] for recent interesting work.

In principle, the processes analyzed in this paper could be utilized as a kind of coherent beam splitter, the first step in a protocol of atom interferometry. It would be very interesting to understand the possibilities and limitations that these systems could have in terms of precision metrology, but this lies beyond the scope of the present work.

Since the whole analysis is based on solving the one-dimensional Gross-Pitaevskii equations, it may be possible that the results presented could be relevant for other physical systems apart from Bose-Einstein condensates, as for example light propagation in optical fibers — see for instance [52] for a recent work which shares some similarities with the set-up of section IV-A.

Acknowledgements

We thank David Nóvoa for helpful discussions. This work was supported by Xunta de Galicia (project 10PXIB383191PR) and by the Univ. Vigo research programme. The work of A. Paredes is supported by the

Ramón y Cajal programme. The work of D. Feijoo is supported by the FPU Ph. D. fellowship programme.

[1] M. H. Anderson, *et al.*, Science **269**, 198 (1995); K. B. Davis, *et al.*, Phys. Rev. Lett. **75**, 3969 (1995).

[2] M. -O. Mewes, *et al.*, Phys. Rev. Lett. **78**, 582 (1997); A. D. Cronin, J. Schmiedmayer, D. E. Pritchard, Rev. Mod. Phys. **81**, 1051-1129 (2009); Y. Shin, et al., Phys. Rev. Lett. **92**, 050405 (2004); T. Schumm, *et al.*, Nature Phys. **1**, 57 (2005).

[3] K. E. Strecker, G.B. Partridge, A.G. Truscott R.G. Hulet, Nature **417**, 150 (2002).

[4] L. Khaykovich, *et al.*, Science **296**, 1290 (2002).

[5] N.G. Parker, A.M. Martin, S.L. Cornish, C.S. Adams, J. Phys. B: At. Mol. Opt. Phys. **41** (2008) 045303.

[6] C. Weiss, Y. Castin, Phys. Rev. Lett. **102**, 010403 (2009).

[7] A.I. Streltsov, O.E. Alon, L.S. Cederbaum, Phys. Rev. A **80**, 043616 (2009).

[8] T.P. Billam, S.L. Cornish, S.A. Gardiner, Phys. Rev. A **83**, 041602 (2011).

[9] U. Al Khawaja, H.T.C. Stoof, New J. Phys. **13**, 085003 (2011).

[10] A.D. Martin, J. Ruostekoski, New J. Phys. **14**, 043040 (2012).

[11] T.P. Billam, S.A. Wrathmall, S.A. Gardiner, Phys. Rev. A **85**, 013627 (2012).

[12] J.L. Helm, T.P. Billam, S.A. Gardiner, Phys. Rev. A **85**, 053621 (2012).

[13] H. Michinel, A. Paredes, M.M. Valado and D. Feijoo, Phys. Rev. A **86**, 013620 (2012).

[14] V. M. Pérez-Garcia, H. Michinel, and H. Herrero, Phys. Rev. A **57**, 3837 (1998).

[15] S. Inouye, *et al.*, Nature **392**, 151 (1998). M. Theis, *et al.*, Phys. Rev. Lett. 93, 123001 (2004).

[16] C. Chin, R. Grimm, P. Julienne and E. Tiesinga, Rev. Mod. Phys. **82**, 12251286 (2010).

[17] L. D. Carr and J. Brand, Phys. Rev. A **70**, 033607 (2004).

[18] S. V. Manakov, Zh. Eksp. Teor. Fiz. 65, 505 (1973) [Sov. Phys. JETP 38, 248 (1974)]

[19] X. Liu, H. Pu, B. Xiong, W.M. Liu and J. Gong, Phys. Rev. A **79**, 013423 (2009).

[20] G. Csire, D. Schumarer and A. Apagyi, Phys. Rev. A **82**, 063608 (2010).

[21] Z.M. He, D.L. Wang, J.W. Ding and X.H.Yan, Eur. Phys. J. D **66**: 139 (2012).

[22] G. Thalhammer, G. Barontini, L. De Sarlo, J. Catani, F. Minardi and M. Inguscio, Phys. Rev. Lett. **100**, 210402 (2008); K. Pilch, A.D. Lange, A. Prantner, G. Kerner, F. Ferlaino. H.-C. Nägerl and R. Grimm, Phys. Rev. A. **79**, 042718 (2009); Th. Best, S. Will, U. Schneider, L. Hackermüller, D. van Oosten, I. Bloch and D.-S. Lühmann, Phys. Rev. Lett. **102**, 030408 (2009).

[23] D. Novoa, B.A. Malomed, H. Michinel and V.M. Pérez-García, Phys. Rev. Lett, **101**, 144101 (2008).

[24] H. Zeng, W. Zhang, F. Lin, Phys. Rev. A **52**, 21552160 (1995).

[25] E. P. Gross, Il Nuovo Cimento **20**, 454-457 (1961); L.P. Pitaevskii, Soviet Physics JETP **13** 451-454 (1961); F. Dalfovo, S. Giorgini, L.P. Pitaevskii, S. Stringari, Rev. Mod. Phys. **71**, 463 (1999).

[26] S. Geltman, Europhys. Lett. **87**, 13001 (2009).

[27] K. Kasamatsu and M. Tsubota, Phys. Rev. A **74**, 013617 (2006).

[28] E.V. Goldstein and P. Meystre, Phys. Rev. A **55**, 2935 (1997), T.S. Raju, P.K. Panigrahi and K. Porsezian, Phys. Rev. A **71**, 035601 (2005), N.G. Berloff, Phys. Rev. Lett. **94**, 120041 (2005), I. Kourakis, P.K. Shukla, M. Marklund and L. Stenflo, Eur. Phys. J. B **46**, 381 (2005).

[29] V.I. Bespalov and V.I. Talanov, JETP Letters-USSR 3-12 (1966), 307.

[30] D. M. Stamper-Kurn, *et al.*, Phys. Rev. Lett. **80**, 2027 (1998).

[31] J. P. Martikainen, Phys. Rev. A **63**, 043602 (2001).

[32] B.D. Esry, C.H. Greene, J. P. Burke, Jr. and J. L. Bohn, Phys. Rev. Lett. **78**, 3594 (1997).

[33] L. D. Carr and J. Brand, Phys. Rev. Lett. **92**, 040401 (2004).

[34] S. Sinha, A.Y. Cherny, D. Kovrizhin, J. Brand, Phys. Rev. Lett. **96**, 030406 (2006).

[35] D.S. Petrov, G.V. Shlyapnikov, J.T.M. Walraven, Phys. Rev. Lett, **85**, 3745 (2000).

[36] V. M. Pérez-García, H. Michinel, J.I. Cirac, M. Lewenstein, P. Zoller, Phys Rev Lett. **77**, 5320 (1996).

[37] S. E. Pollack *et al.*, Phys. Rev. Lett. **102**, 090402 (2009).

[38] T. Schuster *et al.*, Phys. Rev. A **85**, 042721 (2012).

[39] C.J. Myatt, E.A. Burt, R.W. Ghrist, E.A. Cornell, C.E.Wieman, Phys. Rev. Lett. **78**, 586 (1997).

[40] M. Boiti, F. Pempinelli, A.K. Pogrebkov, B. Prinari, Phys. Lett A **285**, 307 (2005). A.M. Pupasov, B.F. Samsonov, SIGMA **1** (2005), 020.

[41] L. D. Landau and E. M. Lifschitz, *Course of Theoretical Physics, Vol.3: Quantum Mechanics*, 3rd ed., sec. 23, Pergamon Press (Oxford), 1991.

[42] I. Kay, H. E. Moses, J. Appl. Phys. **27**, 1503 (1956). J. Lekner, Am. J. Phys. **75**, (12) 1151 (2007).

[43] C. Marzok *et al.*, Phys. Rev. A **79**, 012717 (2009).

[44] J. L. Bohn and P. S. Julienne, Phys. Rev. A **60**, 414-425 (1999). G. Thalhammer, M. Theis, K. Winkler, R. Grimm and J. H. Denschlag , Phys. Rev A **71**, 033404 (2005).

[45] S. B. Papp, J. M. Pino and C. E. Wieman, Phys. Rev. Lett. **101**, 040402 (2008).

[46] N. R. Claussen *et* al., Phys. Rev. A **67**, 060701(R) (2003).

[47] S. L. Cornish, N. R. Claussen, J. L. Roberts, E. A. Cornell, and C. E. Wieman, Phys. Rev. Lett. **85** 1795-1798 (2000).

[48] S. L. Cornish, S. T. Thompson and Carl E. Wieman, Phys. Rev. Lett **96**, 170401 (2006).

[49] K. M. Mertes *et*. al, Phys. Rev. Lett **99**, 190402 (2007).

[50] S. B. Papp and C. E. Wieman, Phys. Rev. Lett. **97**, 180404 (2006).

[51] A. M. Kaufman, B. J. Lester, C. A. Regal, Phys. Rev. X **2**, 041014 (2012).

[52] M. F. Saleh, F. Biancalana, Phys. Rev. A **87**, 043807 (2013).